This research has been co-financed by the European Union (European Social Fund, ESF) and Greek national funds through the Operational Program "Education and Lifelong Learning" of the National Strategic Reference Framework (NSRF), under the grants schemes "Funding of proposals that have received a positive evaluation in the 3rd and 4th Call of ERC Grant Schemes" and the program "Thales"

Gauge/Gravity Duality 2013
Munich, 29 July 2013

Holography and the Chern-Simons diffusion rate

Elias Kiritsis

University of Crete APC, Paris

Bibliography

Based on recent work with:

Umut Gursoy, (Utrecht), Ioannis Iatrakis (Crete), Francesco Nitti, (APC), Andy O'Bannon (Cambridge) arXiv:1212.3894 [hep-ph]

and based also on past work with:

- Umut Gursoy, (Utrecht), Liuba Mazzanti (Utrecht), Francesco Nitti, (APC)

arXiv:0903.2859 [hep-th]

arXiv:0707.1349 [hep-th]

Introduction: Instantons

• Instantons are important topological semiclassical configurations of $SU(N_c)$ YM theory.

• They are responsible for the existence of an infinite number of degenerate vacua, and a new coupling constant (the instanton angle θ that breaks the CP symmetry in YM).

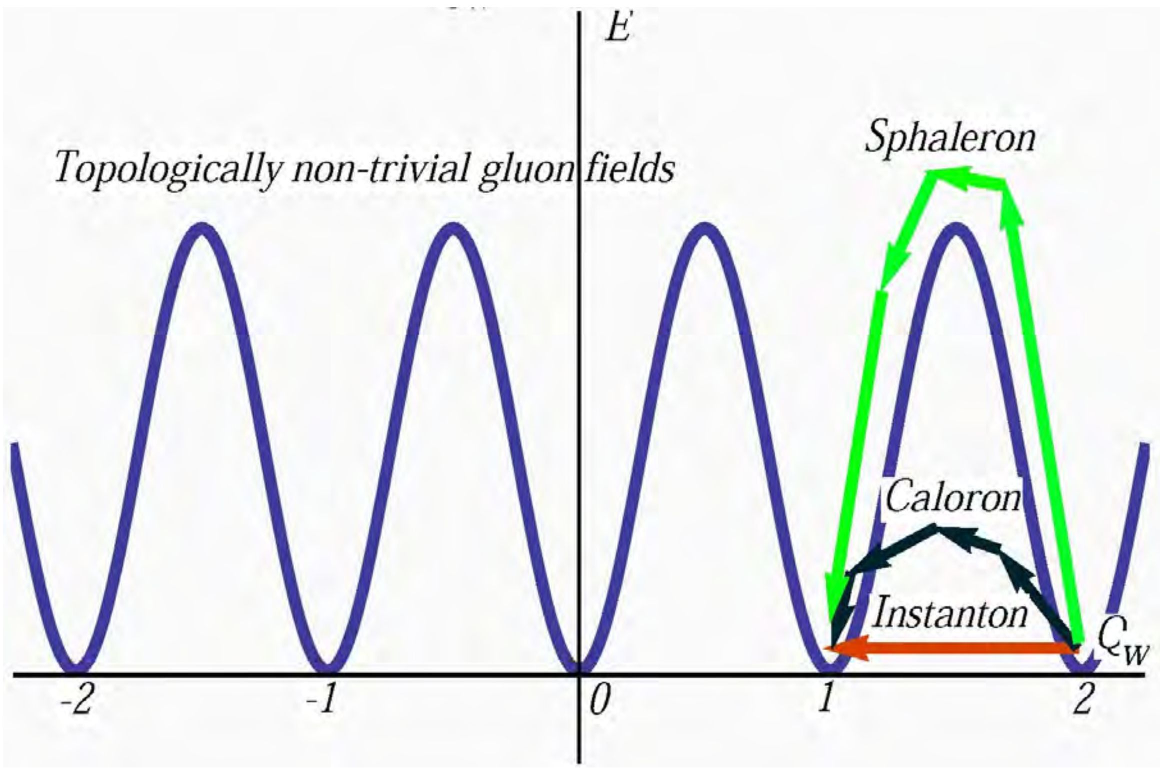

• When they can be treated as a dilute instanton gas, their contributions are exponentially small in perturbation theory,

$$\sim \quad e^{-\frac{8\pi^2\ N_c}{\lambda}}$$

• However, instantons have a size, and large instantons are affected by the IR coupling of the YM Theory that is strong.

• This is the reason that, although we know how to calculate with individual instantons, the dynamical contributions of instantons to many YM processes are un-calculable.

Instantons at large N_c

• Because the instanton factor $e^{-\frac{8\pi^2}{\lambda} N_c}$ is exponentially suppressed with N_c, instanton effects should be exponentially small in the large-N_c limit.

• Veneziano-Witten, solving the η'-puzzle, pointed out that this is sometimes **false**.

• In QCD, at T=0, the instanton charge is effectively continuous, the instantons cannot be treated like a gas (because large instantons dominate), and instanton effects are NOT exponentially suppressed, but only power suppressed, like other dynamical effects.

Witten '79, Veneziano, '79

• In particular the mass of the η' (the 9-th would-be Goldstone boson of $U(1)_A$ in QCD) is

$$M_{\eta'} \sim \frac{N_f}{N_c} \ \Lambda_{QCD}$$

The $U(1)_A$ anomaly

• The most important role of instantons is to violate the $U(1)_A$ charge conservation in QCD

$$J_5^\mu \;=\; \sum_{i=1}^{N_f} \;\overline{\psi}_i \;\; \gamma^\mu \;\; \gamma^5 \;\; \psi_i$$

$$\partial_\mu J_5^\mu = -\frac{N_f}{16\pi^2}\;\epsilon^{\mu\nu\rho\sigma}\;\mathbb{T}r F_{\mu\nu}F_{\rho\sigma} \;\;=\;\; -\frac{N_f}{8\pi^2}\;\mathbb{T}r F\wedge F\,.$$

• A related number is the Chern-Simons number N_{CS} that characterizes distinct vacua of $SU(N_c)$ YM which cannot be connected with small gauge transformations. It is defined at fixed time, spatial (3d) slices as

$$N_{CS}\equiv\frac{1}{8\pi^2}\int_{\partial M}d^3x\,\epsilon_{ijk}\,\mathbb{T}r\left[A_i\partial_jA_k-\frac{2ig}{3}A_iA_jA_k\right]$$

where $i,j,k=1,2,3$.

The CS diffusion rate

• The Chern-Simon diffusion rate, Γ_{CS}, is the rate of change of ΔN_{CS} per unit 4-volume and is given by the two-point function of $q(x^\mu)$,

$$\Gamma_{CS} \equiv \frac{\langle(\Delta N_{CS})^2\rangle}{Vt} = \int d^4x\ \langle q(x^\mu)q(0)\rangle_{\text{symmetric}}$$

• In equilibrium states with finite temperature, Γ_{CS} is given in terms of $G_R(\omega,\vec{k})=$ Fourier transform of the retarded Green function of $q(x^\mu)$ by:

$$\Gamma_{CS} = -\lim_{\omega\to 0} \frac{2T}{\omega}\ \text{Im}\, G_R(\omega,\vec{k}=0)\,,$$

• Single instanton background contributions to Γ_{CS} are exponentially suppressed.

• Γ_{CS} can be generated by thermal fluctuations in finite temperature states. Those excite sphaleron configurations which produce non-zero Γ_{CS} upon decay.

• Since $q(x)$ is a total derivative, Γ_{CS} is identically zero in perturbation theory.

• A finite value for Γ_{CS} in QCD, signals the creation of net chirality bubbles because of the anomaly of the axial current. These are domains of more left-handed than right-handed quarks or the opposite.

The chiral magnetic effect

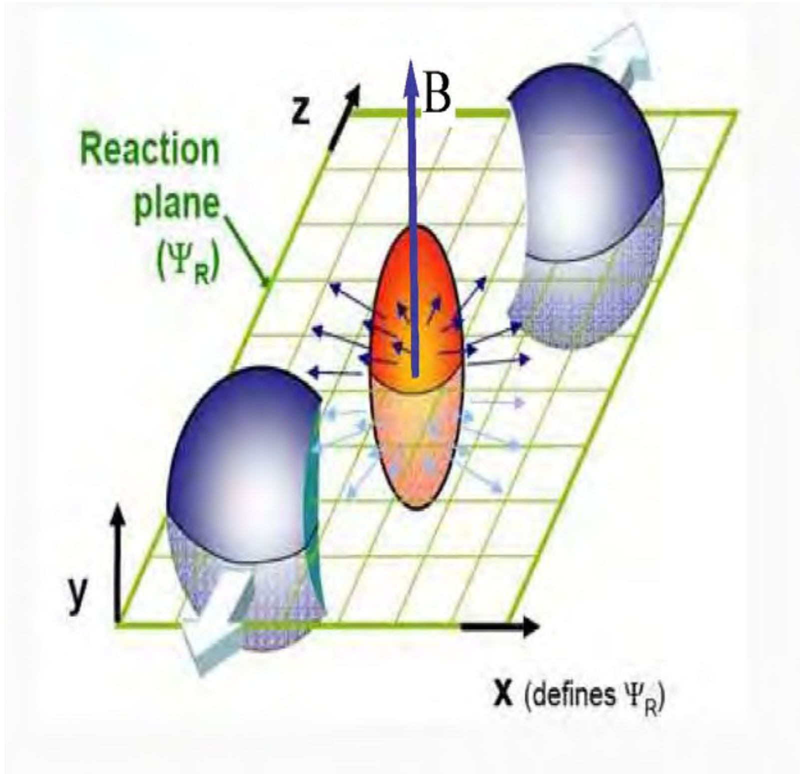

- The electric current generates a magnetic field, $B \sim \gamma Z e \frac{b}{R^3} \sim 10^{18}$ (10^{19}) at RHIC (LHC). Or $eB \sim 5 - 15\ m_\pi^2$.

- In neutron stars $B \sim 10^{10} - 10^{13}$ $Gauss$. In magnetars, $B \sim 10^{15}$ $Gauss$

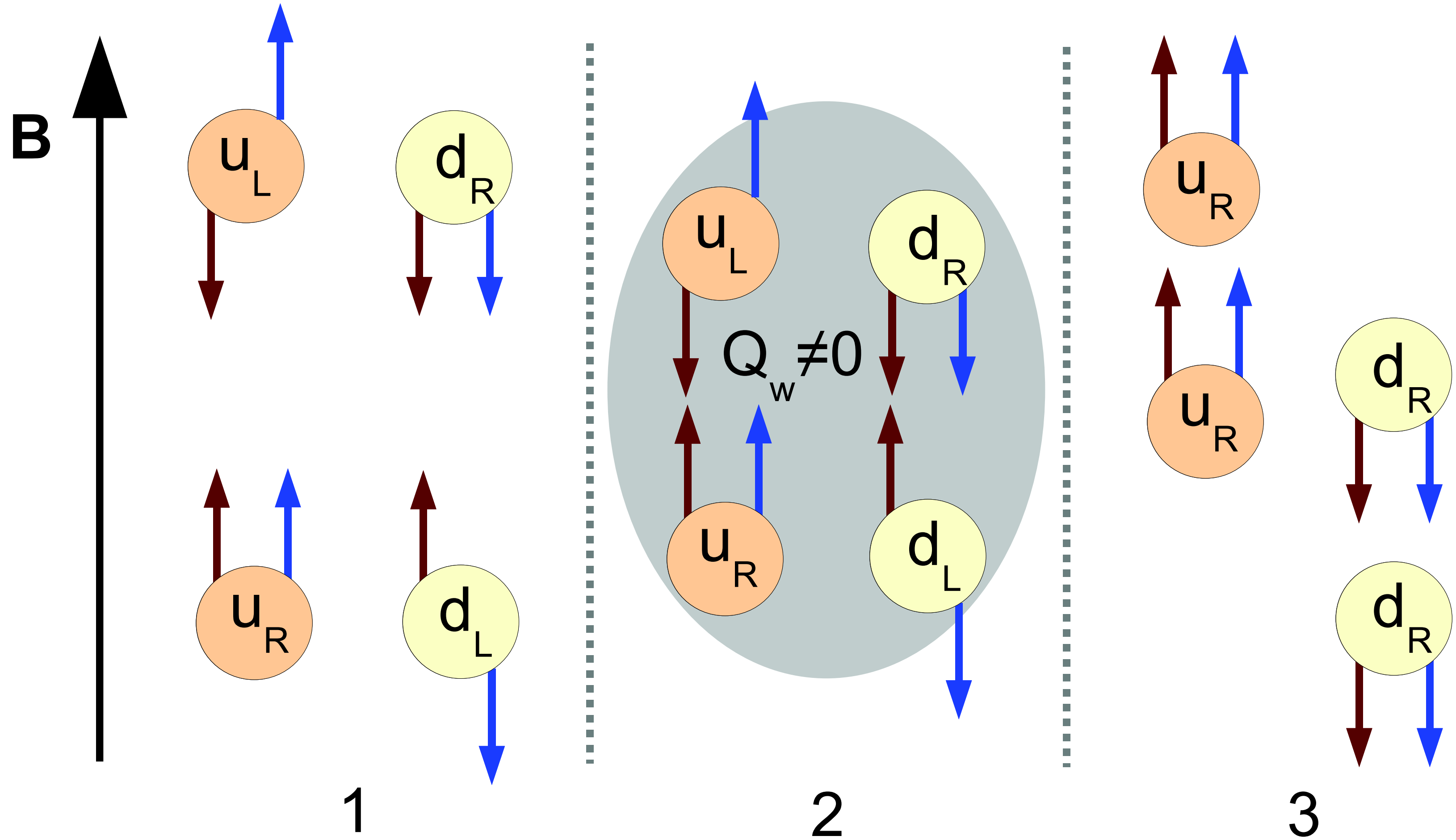

• A magnetic field, separates spatially the electric charge of left-moving fermions (blue is spin, brown is momentum).

• Fluctuations of axial charge due to sphalerons, and the strong magnetic field, will generate, charge asymmetry on an event-by-event basis.

What is known about Γ_{CS}?

• Γ_{CS} is a crucial ingredient for the Chiral magnetic effect. The bigger it is, the bigger are the fluctuations of the chiral asymmetry.

• Γ_{CS} is a non-perturbative, (Minkowskian) transport coefficient.

• At high enough temperature, using classical field dynamics, hard thermal loop resummation and (and Bödeker's effective theory). It is reliable for $(\alpha_s \ll 1, \frac{1}{\log\frac{1}{\alpha_s}} \ll 1)$

$$\Gamma_{CS} = 0.21 \quad \frac{N_c g^2 T}{m_D^2}\left(\log\frac{m_D}{\gamma} + 3.041\right)\frac{N_c^2 - 1}{N_c^2}\ (N_c\ \alpha_s)^5\ T^4$$

$$m_D^2 = \frac{2N_c + N_f}{6} g^2 T^2 \quad , \quad \gamma = \frac{N_c g^2 T}{4\pi}\left(\log\frac{m_D}{\gamma} + 3.041\right) \quad , \quad a_s = \frac{g^2}{4\pi}$$

Giudice+Shaposhnikov, '93, Moore, '97, '00, Moore+Tassler, '10

• $N = 4$ sYM calculation

Son+Starinets, '02

$$\Gamma_{CS} = \frac{\lambda^2}{2^8\pi^3}\ T^4$$

• What is Γ_{CS} in YM?

IHQCD

• IHQCD is a specially chosen 5d Einstein dilaton model (with two phenomenological parameters in $V(\lambda)$)

$$S = M_p^3 N_c^2 \int d^5x \sqrt{-g} \left[R - \frac{4}{3}\frac{(\partial\lambda)^2}{\lambda^2} + V(\lambda) \right]$$

where $\lambda = e^{\phi}$ and $(M_p \ell)^3 = 45\pi^2$.

Gursoy+Kiritsis+Nitti, '07

$$V(\lambda) = \frac{12}{\ell^2}\left[1 + \sum_{n=1}^{\infty} V_n \lambda^n\right] \quad , \quad \lambda \to 0$$

$$V(\lambda) \sim \lambda^{\frac{4}{3}} \sqrt{\log\lambda} + \cdots \quad , \quad \lambda \to \infty$$

• The model reproduces correctly the spectra of 0^{++} and 2^{++} glueballs, as well as the finite temperature thermodynamics.

• It has confinement, a mass gap and asymptotically linear trajectories: $m_n^2 \sim n$.

The instanton density in IHQCD

• The instanton density $q(x)$ is dual to an axion field, $a(x,r)$. In N=4 sYM this is the usual IIB axion in ten dimensions.

• The most general action for the axion compatible with the symmetries of the instanton density is

$$S_a = \frac{M_p^3}{2}\int d^5x\sqrt{g}\ \ Z(\lambda)\ (\partial a)^2 + \mathcal{O}\left(\frac{(\partial a)^4}{N_c^2}\right)$$

• There is no axion potential and therefore the symmetry $a \to a + constant$ is exact.

• S_a is of order $\mathcal{O}(N_c^{-2})$ compared with the IHQCD action.

$$\text{UV}\quad \lambda \to 0 \qquad Z(\lambda) = Z_0\left[1 + \sum_{n=1}^{\infty} c_n\lambda^n\right]$$

$$\text{IR}\quad \lambda \to \infty \quad Z(\lambda) \sim c_4\lambda^4 + \cdots \quad , \quad \lim_{n\to\infty}\frac{m_n^2(0^{-+})}{m_n^2(0^{++})} = 1$$

Gursoy+Kiritsis+Mazzanti+Nitti, '09

The θ flow

- The axion background solution $a(r)$ can be interpreted as a "running" θ-angle

- This is in accordance with the absence of UV divergences (all correlators $\langle Tr[F\wedge F]^n\rangle$ are UV finite), and Seiberg-Witten type solutions.

- The equation of motion is

$$\ddot{a}+\left(3\dot{A}+\frac{\dot{Z}(\lambda)}{Z(\lambda)}\right)\dot{a}=0 \quad , \quad ds^2=e^{2A(r)}(dr^2+dx^\mu dx_\mu)$$

- The metric $A(r)$ and $\lambda(r)$ are taken from the leading order solution.

- The full solution is

$$a(r)=\theta_{UV}+2\pi k+C\int_0^r dr\frac{e^{-3A}}{Z(\lambda)} \quad , \quad C=\langle q(x)\rangle=\frac{1}{16\pi^2}\langle Tr[F\wedge F]\rangle$$

- $a(r)$ is a running effective θ-angle. Its running is non-perturbative,

$$a(r)\sim r^4\sim e^{-\frac{4}{b_0\lambda}}$$

- The vacuum energy is

$$E(\theta_{UV}) = -\frac{M_p^3}{2}\int d^5x\sqrt{g}\ Z(\lambda)\ (\partial a)^2 = -\frac{M_p^3}{2} C a(r)\ \Big|_{r=0}^{r=\infty}$$

- Consistency with the $\theta \to -\theta$ symmetry of YM requires to impose that $a(\infty) = 0$. This determines the solution

Witten, '79

$$C = \langle q(x)\rangle = -\frac{\theta_{UV} + 2\pi k}{\int_0^\infty dr \frac{e^{-3A}}{Z(\lambda)}}$$

$$E(\theta_{UV}) = E_{IHQCD} + \frac{M_p^3}{2}\text{Min}_k\ \ \frac{(\theta_{UV} + 2\pi k)^2}{\int_0^\infty \frac{dr}{e^{3A}Z(\lambda)}}$$

- The topological susceptibility χ is given by

$$E(\theta) = N_c^2 E_0 + \frac{1}{2}\chi\ \theta^2 + \mathcal{O}\left(\frac{\theta^4}{N_c^2}\right) \quad , \quad \chi = \frac{M_p^3}{\int_0^\infty \frac{dr}{e^{3A}Z(\lambda)}}$$

- The simplest parametrization of $Z(\lambda)$ consistent with asymptotics is

$$Z(\lambda) = Z_0\left(1 + c_4\lambda^4\right)$$

- Z_0 can be determined from the topological susceptibility (lattice, $\chi \simeq (191\text{MeV})^4$), and c_4 from the lowest 0^{-+} glueball mass (lattice, $\frac{m_{0^{-+}}}{m_{0^{++}}} = 1.50$). The predicted next mass agrees well with lattice ($\frac{m_{0^{*-+}}}{m_{0^{++}}} = 2.11$).

The 2-point function of $q(x)$

• We now proceed to calculate the 2-point function $\langle q(x)q(0)\rangle$ at finite temperature, $T \geq T_c$.

• The linear fluctuation equation of the axion (in Fourier space) is considered in the black hole background, $ds^2 = e^{2A}\left(\frac{dr^2}{f} - f dt^2 + dx^i dx_i\right)$,

$$\left[\frac{1}{Z(\lambda)\sqrt{-g}}\partial_r\left(Z(\lambda)\sqrt{-g}\, g^{rr}\partial_r\right) - g^{\mu\nu}k_\mu k_\nu\right]\delta\alpha(r,k^\mu) = 0\,,$$

with in-going wave boundary conditions at the horizon.

• The on shell action of the fluctuation is

$$S_\alpha^{\text{on-shell}} = \int \frac{d^4k}{(2\pi)^4}\, a(-k^\mu)\,\mathcal{F}(r,k^\mu)\,a(k^\mu)\Big|_0^{r_h}\,,$$

$$\mathcal{F}(r,k^\mu) \equiv -M_p^3\,\delta\alpha(r,-k^\mu)\,Z(\lambda)\,\sqrt{-g}\,g^{rr}\,\partial_r\delta\alpha(r,k^\mu)/2$$

• The AdS/CFT dictionary yields that the retarded Green's function is

$$\hat{G}_R(\omega,\vec{k}) = -2\lim_{r\to 0}\mathcal{F}(r,k^\mu).$$

The calculation of the CS diffusion rate

- We can calculate directly the IR limit of G_R and therefore Γ_{CS} to be

$$\frac{\Gamma_{CS}}{sT/N_c^2} = \frac{Z(\lambda_h)}{2\pi},$$

which has implicit dependence on T through $Z(\lambda_h)$. λ_h is the value of the dilaton at the black hole horizon.

- On the large black hole branch, $\Gamma_{CS}/(sT/N_c^2)$ is bounded from below by its value in the $T \to \infty$ limit,

$$\lim_{T\to\infty} \frac{\Gamma_{CS}}{sT/N_c^2} = \frac{Z_0}{2\pi}$$

.

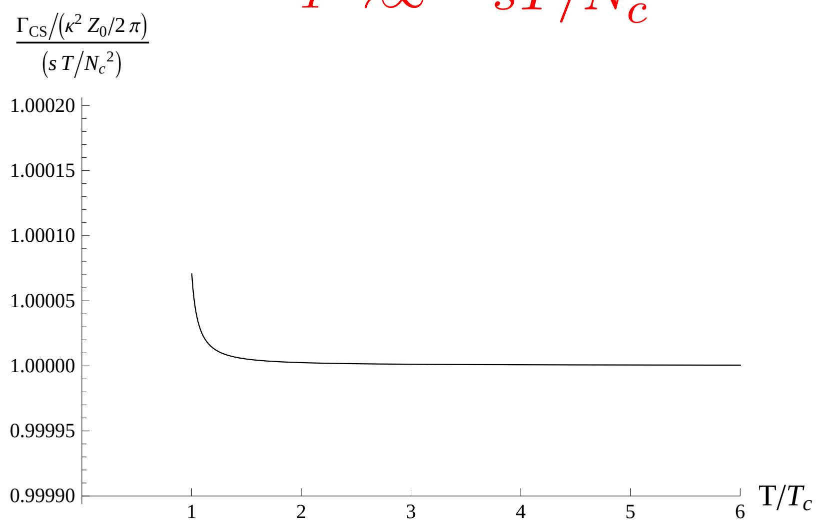

• The previous calculation of Γ_{CS} is not reliable because:
(a) The parametrization was crude
(b) $\lambda_h < 1$

• The largest polynomial correction to $Z(\lambda)$ for small values of λ will come from linear terms so we reparametrize $Z(\lambda)$ as

$$Z(\lambda) = Z_0 \left(1 + c_1 \lambda + c_4 \lambda^4\right)$$

• To constrain c_1 we will demand that our holographic results for the axial glueball masses fall within one σ of the lattice values for the two first 0^{-+} glueball masses

$$0 < c_1 < 5 \quad , \quad 0.06 < c_4 < 50$$

• Simple non-monotonic $Z(\lambda)$s with the desired asymptotics, produce glueball masses that deviate from lattice results more than 10%.

• This implies that the bound $\frac{\Gamma_{CS}}{sT/N_c^2} \leq \frac{Z_0}{2\pi}$ is always valid.

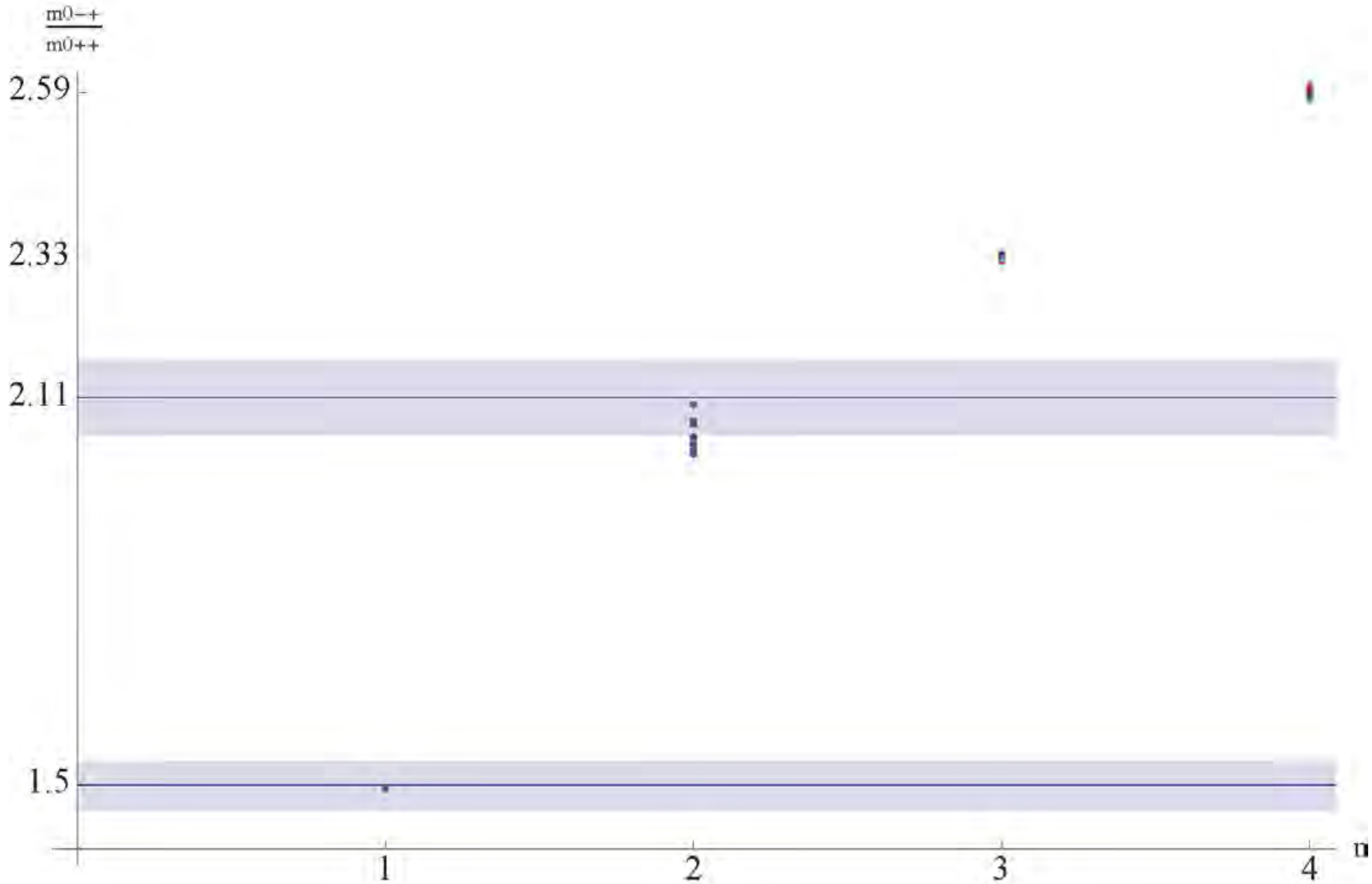

IHQCD masses of the 0^{-+} glueball states with excitation number n, normalized to the 0^{++} mass for various (c_1, c_4). From the top (red) dots to the bottom (blue) dots: $(c_1, c_4) = (0, 0.26), (0.5, 0.87), (1, 2.2), (5, 24), (10, 75$
The two horizontal blue lines with surrounding blue bands indicate the results and errors, respectively, of the large-N YM lattice masses of the lowest and first excited states, $n = 1$ and $n = 2$, (Morningstar-Peardon).

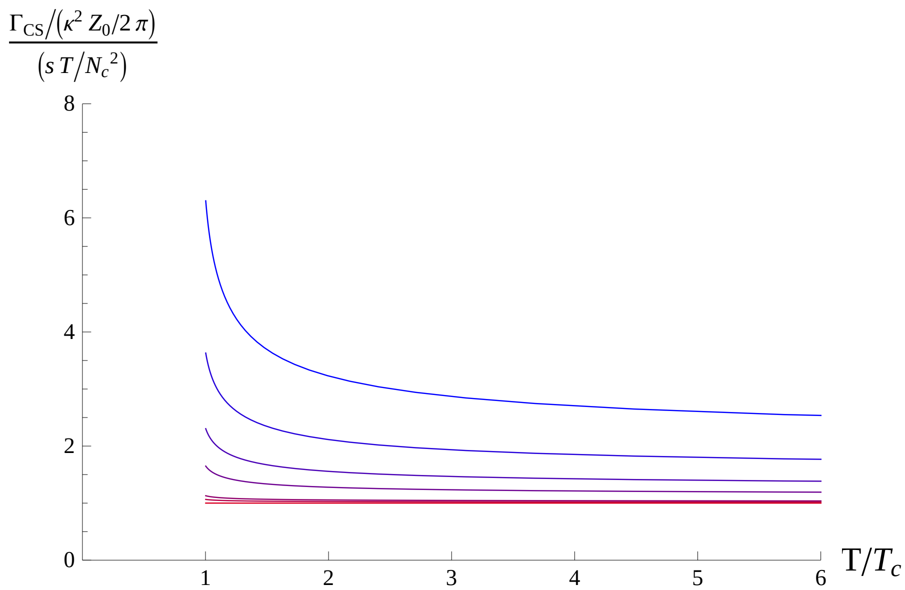

,
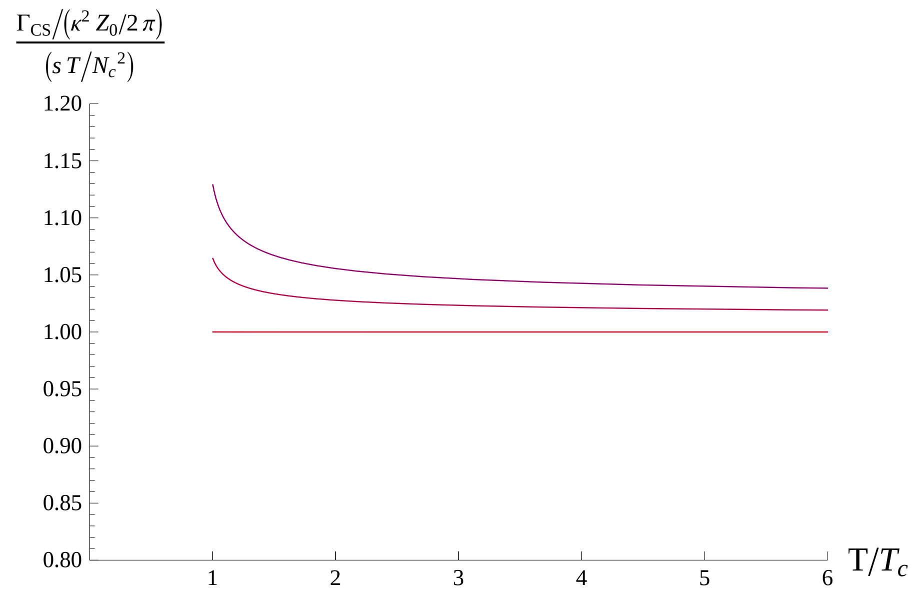

(a) The numerical result for $\Gamma_{CS}/(sT/N_c^2)$, normalized to the $T \to \infty$ value $\kappa^2 Z_0/2\pi$, as functions of T/T_c, for different values of the parameters (c_1, c_4). From the bottom (red) curve to the top (blue) curve, $(c_1, c_4) = (0, 0.26), (0.5, 0.87), (1, 2.2), (5, 24), (10, 75), (20, 230), (40, 600)$. (b) Close-up of the curves for (from bottom to top) $(c_1, c_4) = (0, 0.26), (0.5, 0.87), (1, 2.2)$.

• A numerical estimate of Γ_{CS} near the confinement-deconfinement phase transition is

$$\frac{\Gamma_{CS}(T_c)}{T_c^4} = 0.31 \times \frac{Z(\lambda_c)}{2\pi} \quad > \quad 0.31 \times \frac{Z_0}{2\pi} \quad = \quad 1.64\,,$$

where we have used the lattice result for the entropy density, $s(T_c) = 0.31 N_c^2 T_c^3$, (Lucini-Teper-Wenger).

• At 1 σ an upper bound can also be set to $\Gamma_{CS}(T_c)$. In total

$$1.64 \quad \leq \quad \frac{\Gamma_{CS}(T_c)}{T_c^4} \quad \leq \quad 2.8$$

• We may compare this range of values with the N=4 result taking the standard values, $\lambda \simeq 6\pi$ to get a result that is at least 40 times smaller.

$$N = 4 \;\; \text{sYM} \quad : \quad \frac{\Gamma_{CS}(T)}{T^4} \quad \simeq \quad 0.045$$

• A naive extrapolation of the Moore-Tassler high temperature formula to $\alpha_s = 0.5$, gives the right order of magnitude,

$$\frac{\Gamma_{CS}^{MT}(T_c)}{T_c^4} \quad = \quad 30\alpha_s^5 \quad \simeq \quad 1 \tag{1}$$

The CS correlator

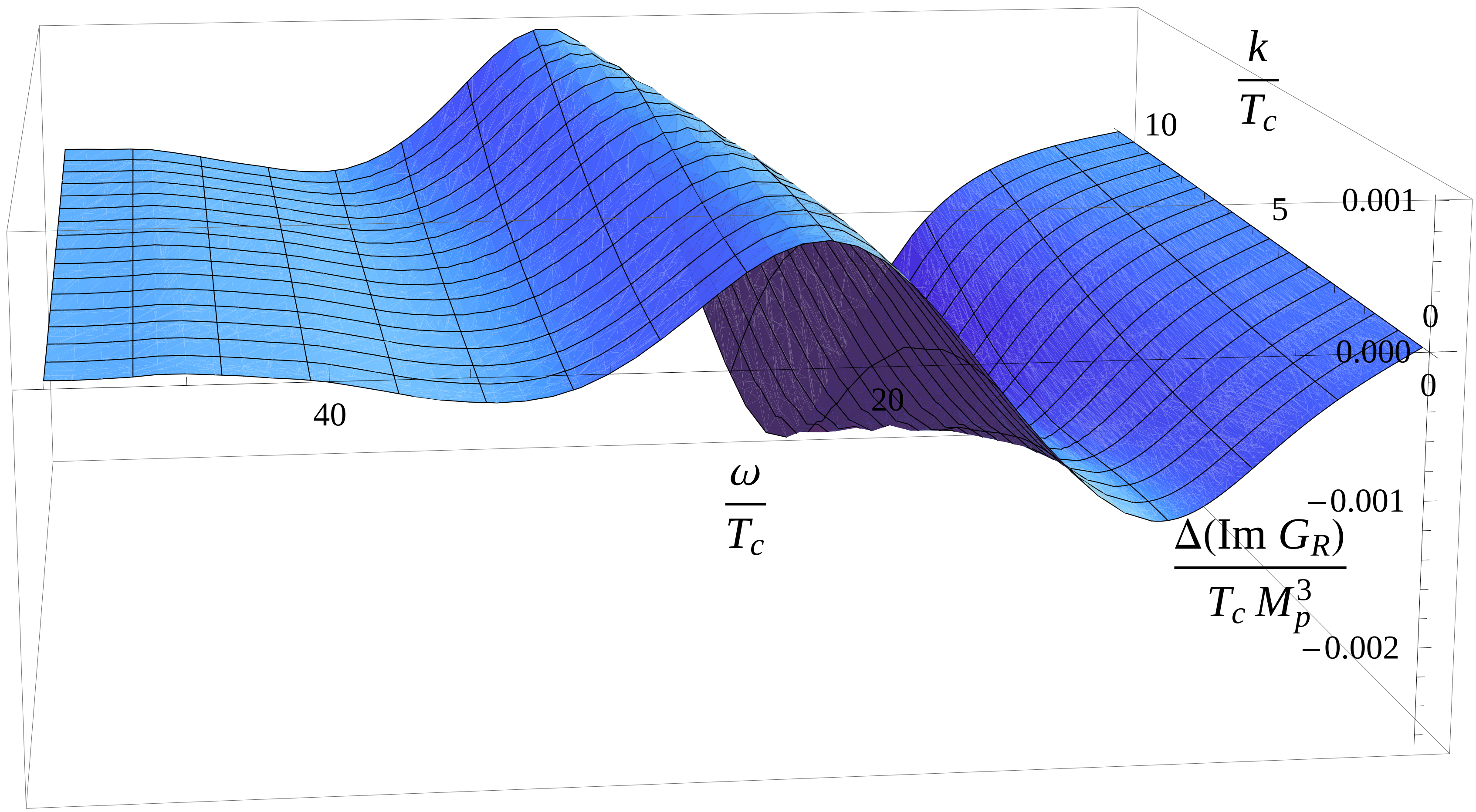

Our numerical results for $\Delta\mathrm{Im}\, G_R(\omega, \vec{k} = 0; T_c, 2T_c)/(T_c M_p^3)$ as a function of ω/T_c and $|\vec{k}|/T_c$. As $|\vec{k}|$ increases up to $|\vec{k}|/T_c \approx 10$, the largest peak shifts from $\omega/T_c \approx 22$ up to $\omega/T_c \approx 30$. The width of the peak changes very little.

Outlook

• The Chern-Simons diffusion rate seems to be non-negligible in QCD and is bounded below.

• CP-odd phenomena above T_c seem to be controlled by a long lived excitation that has the same order of magnitude mass as the 0^{-+} glueball.

• Fixing better $Z(\lambda)$ by the fitting to a lattice calculation of the Euclidean 2-point function of $q(x^\mu)$ is an important future plan.

• Calculate Γ_{CS} in a model which incorporates the flavor degrees of freedom as well (V-QCD).

• The currents which appear in chiral magnetic effect can be calculated holographically upon addition of the flavor in the pure glue background. In this case, a vacuum state with a magnetic field and net chirality should be constructed.

.

Thank you

This research has been co-financed by the European Union (European Social Fund, ESF) and Greek national funds through the Operational Program "Education and Lifelong Learning" of the National Strategic Reference Framework (NSRF), under the grants schemes "Funding of proposals that have received a positive evaluation in the 3rd and 4th Call of ERC Grant Schemes" and the program "Thales"

European Union
European Social Fund

OPERATIONAL PROGRAMME
EDUCATION AND LIFELONG LEARNING
investing in knowledge society
MINISTRY OF EDUCATION & RELIGIOUS AFFAIRS, CULTURE & SPORTS
MANAGING AUTHORITY

NSRF
2007-2013
programme for development
EUROPEAN SOCIAL FUND

Co-financed by Greece and the European Union

Changes of N_{CS}

- The change of N_{CS} during a dynamical process is given by

$$\Delta N_{CS} = \int d^4x \quad q(x^\mu)$$

$$q(x^\mu) \equiv \frac{1}{16\pi^2} \int_M \mathbb{T}r\,[F \wedge F] = \frac{1}{32\pi^2} \epsilon^{\mu\nu\rho\sigma} \mathbb{T}r F_{\mu\nu} F_{\rho\sigma}\,.$$

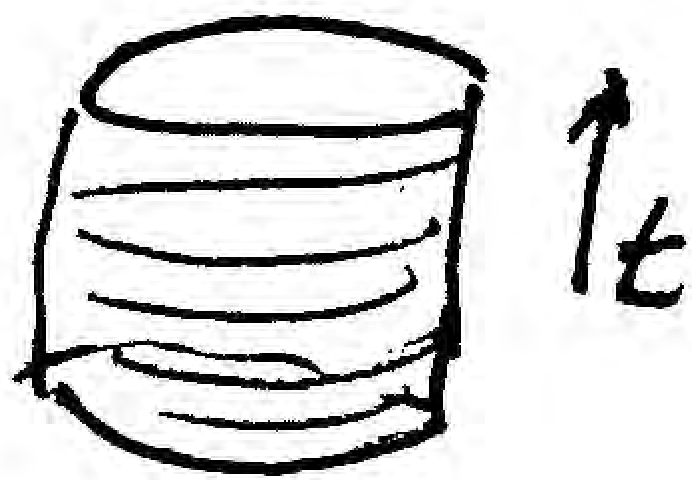

- We conclude that instantons mediate the changes of axial U(1) charge.

$$\Delta N_5 = (N_L - N_R)|_{t=\infty} \quad - \quad (N_L - N_R)|_{t=-\infty} = 2N_f \quad \Delta N_{CS}\,.$$

• In a thermal plasma, such fluctuations of axial U(1) number are controlled by a Langevin-like process

$$\frac{d(\Delta N_5)}{dt} = -\xi_{CS} \;\; \Delta N_5 + \eta(t) \quad , \quad \langle \eta(t)\eta(t')\rangle \simeq \Gamma_{CS}\delta(t-t')$$

where Γ_{CS} is the Chern-Simons diffusion rate.

• As usual, the white-noise correlation is controlled by the symmetric correlator while the friction coefficient ξ_{CS} is controlled by the retarded correlator.

• Consider now the transition amplitude, A, from a state $|\psi_1(t_1)\rangle$ to $|\psi_2(t_2)\rangle$ times the change in axial number

$$A\,\Delta N_5 = 2\int d^4x \langle \psi_2|q(x)|\psi_1\rangle$$

Taking the square of the above equation, summing over all possible $|\psi_2(t_2)\rangle$ and using the completeness relation $\mathbb{I} = \sum |\psi_2\rangle\langle\psi_2|$ we obtain

$$\langle (\Delta N_5)^2\rangle = 4\int \; d^4x \; d^4y \; \langle \psi_1| \; q(x) \; q(y) \; |\psi_1\rangle$$

RETURN

• The Chern-Simon diffusion rate, Γ_{CS}, is the rate of change of ΔN_{CS} per unit 4-volume and is given by the two-point function of $q(x^\mu)$,

$$\Gamma_{CS} \equiv \frac{\langle (\Delta N_{CS})^2 \rangle}{Vt} = \int d^4x \ \langle q(x^\mu) q(0) \rangle_{\text{symmetric}}$$

• In equilibrium states with finite temperature, Γ_{CS} is given by

$$\Gamma_{CS} = 2T \ \ \xi_{CS} = - \lim_{\omega \to 0} \ \frac{2T}{\omega} \ \ \text{Im}\, G_R(\omega, \vec{k} = 0)\,,$$

where $G_R(\omega, \vec{k})=$ Fourier transform of the retarded Green function of $q(x^\mu)$.

• Single instanton background contributions to Γ_{CS} are exponentially suppressed.

• Γ_{CS} can be generated by thermal fluctuations in finite temperature states. Those excite sphaleron configurations which produce non-zero Γ_{CS} upon decay.

• Since $q(x)$ is a total derivative, Γ_{CS} is identically zero in perturbation theory.

• Finite Γ_{CS} in QCD, signals the creation of net chirality bubbles (domains of more left-handed than right-handed quarks or the opposite) because of the anomaly of the axial current.

The θ RG flow

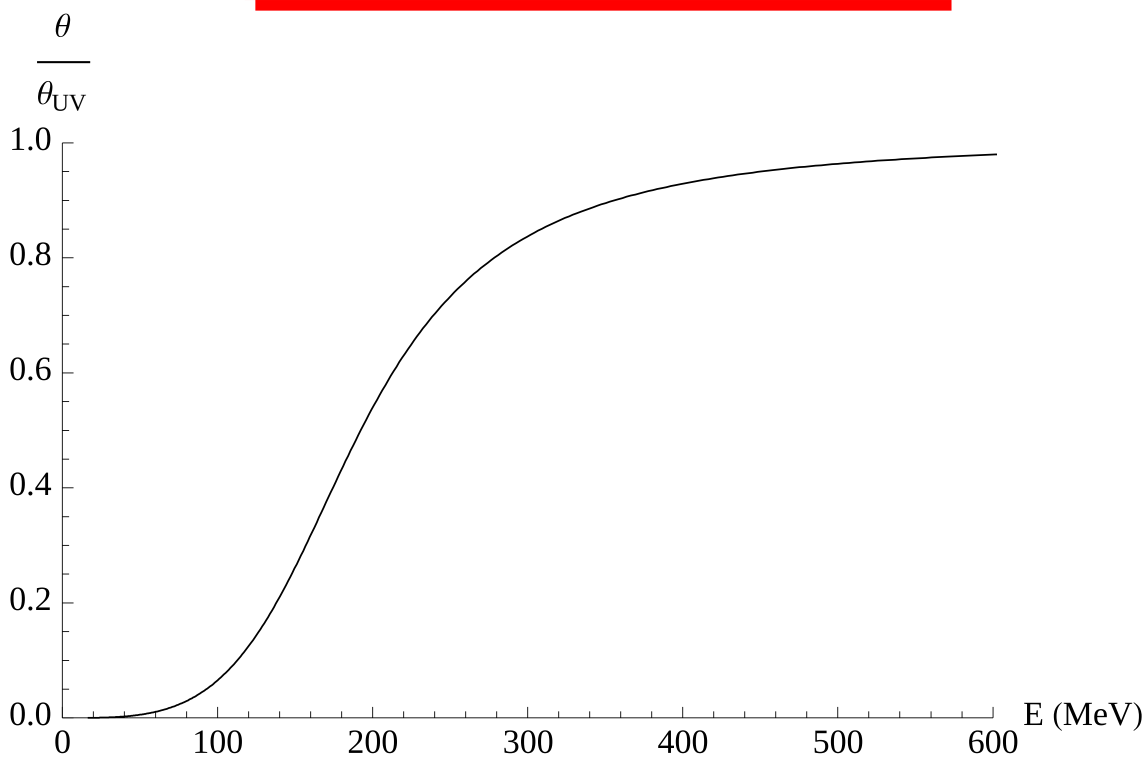

- The effective θ vanishes in the IR. $q(r)$ is a marginally-irrelevant operator.

- We have taken: $Z(\lambda) = Z_0(1 + c_4\lambda^4) \simeq \frac{133}{4}(1 + 0.26\lambda^4)$

- The effective θ-angle "runs" also in the D4 model for QCD, and also vanishes in the IR $\theta(U) = \theta(1 - U_0^3/U^3)$

The CS spectral function

• We now calculate the axion spectral function $\mathrm{Im} G_R(\omega, \vec{k})$ for non-zero ω and $|\vec{k}|$. We first set $\vec{k} = 0$

• For small ω, the axion fluctuation equation yields $\mathrm{Im}\, G_R(\omega, \vec{k} = 0) \propto \omega$.

• For large ω, we expect $\mathrm{Im}\, G_R(\omega, \vec{k} = 0) \propto \omega^4$ because the theory is conformally invariant in the UV and $q(x^\mu)$ has dimension four.

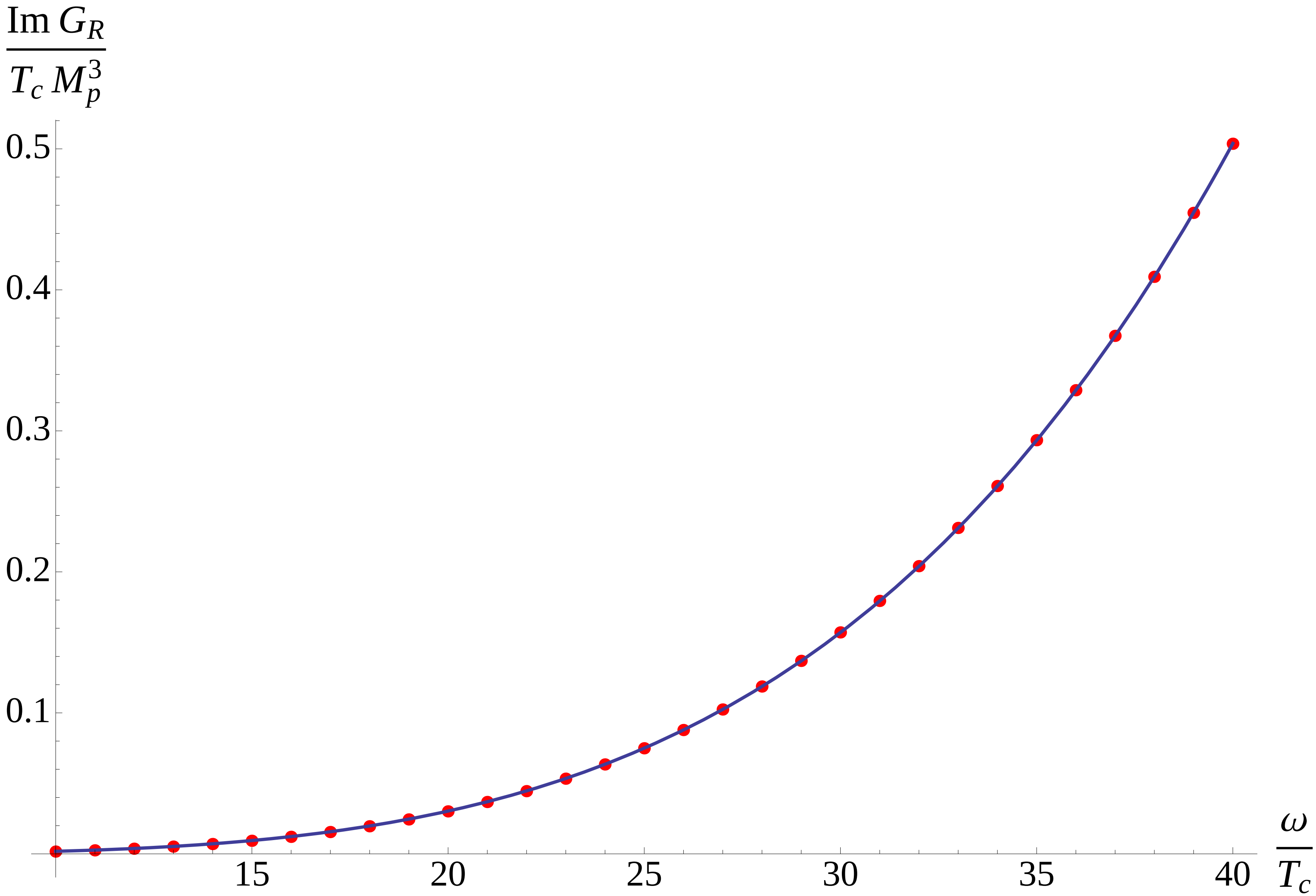

$\mathrm{Im}\, G_R(\omega, \vec{k} = 0)/(T_c M_p^3)$ as a function of ω/T_c, at T_c. The red dots are our numerical results that match the solid blue curve, $(1.6 \times 10^{-7}) \times (\omega/T_c)^{4.051}$, which is the expected large ω behavior of the spectral function.

• The ω^4 scaling of $\text{Im}\, G_R(\omega, \vec{k} = 0)$ at large ω comes from the UV (free) part of the two-point function.

• It overwhelms peaks in $\text{I}m\, G_R(\omega, \vec{k})$, rendering them practically invisible.

• To eliminate the large-ω divergence we compute $G_R(\omega, \vec{k})$ at two different temperatures, T_1 and T_2, and then take the difference,

$$\Delta G_R(\omega, \vec{k}; T_1, T_2) \equiv G_R(\omega, \vec{k})\Big|_{T_2} - G_R(\omega, \vec{k})\Big|_{T_1} .$$

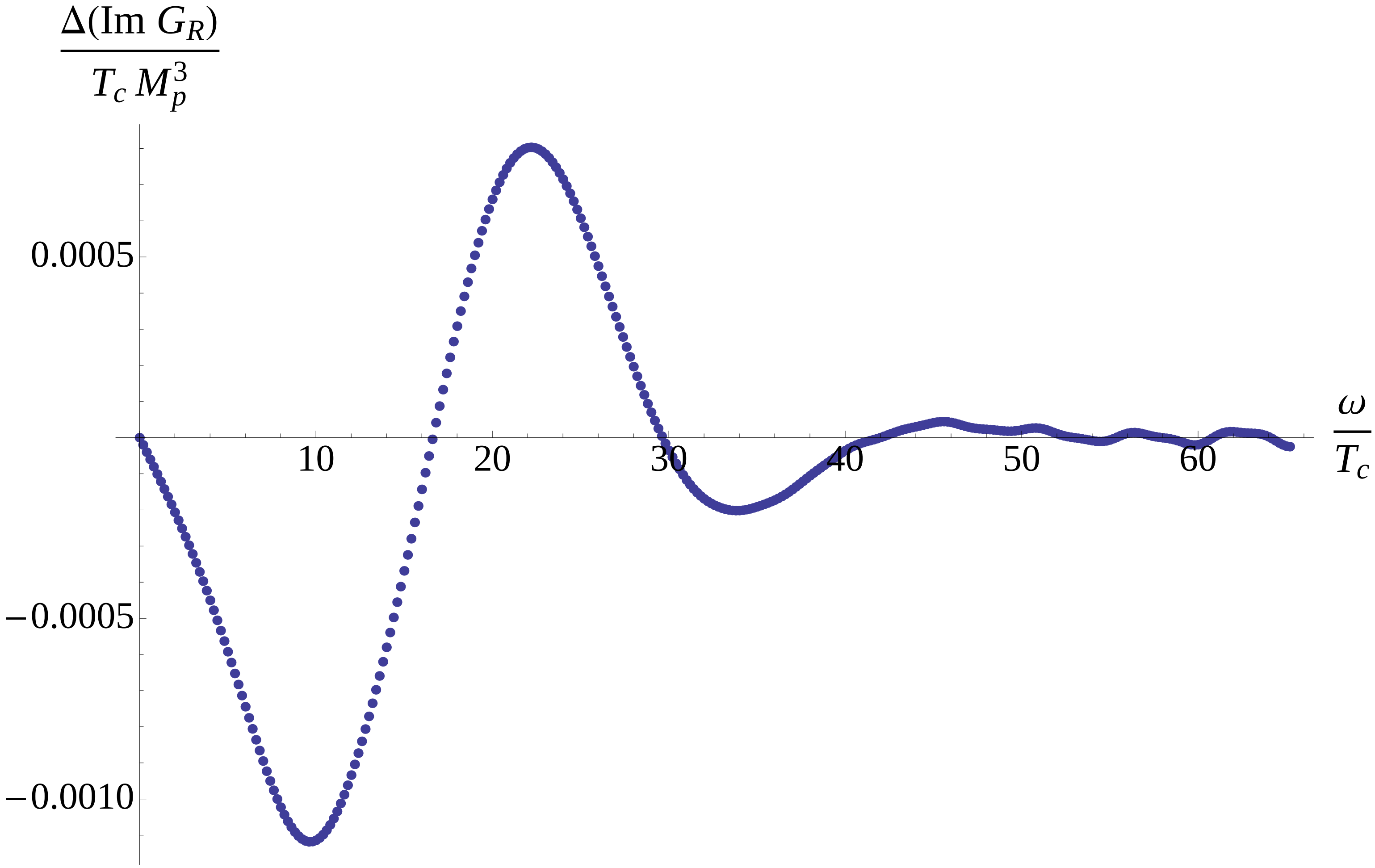

The difference $\Delta \text{Im}\, G_R(\omega, \vec{k} = 0; T_c, 2T_c)/(T_c M_p^3)$ as a function of ω/T_c. The difference goes to zero as $\omega/T_c \to \infty$. The prominent minimum at $\omega/T_c \approx 10$ and maximum at $\omega/T_c \approx 22$ indicate a shift in spectral weight with increasing T, possibly from the motion of a peak in the spectral function. There is a peak at $\omega \simeq 20T_c \simeq 1600$MeV and width $\sim 10T_c \sim 1300$MeV.

Comparison with lattice data (Meyer)

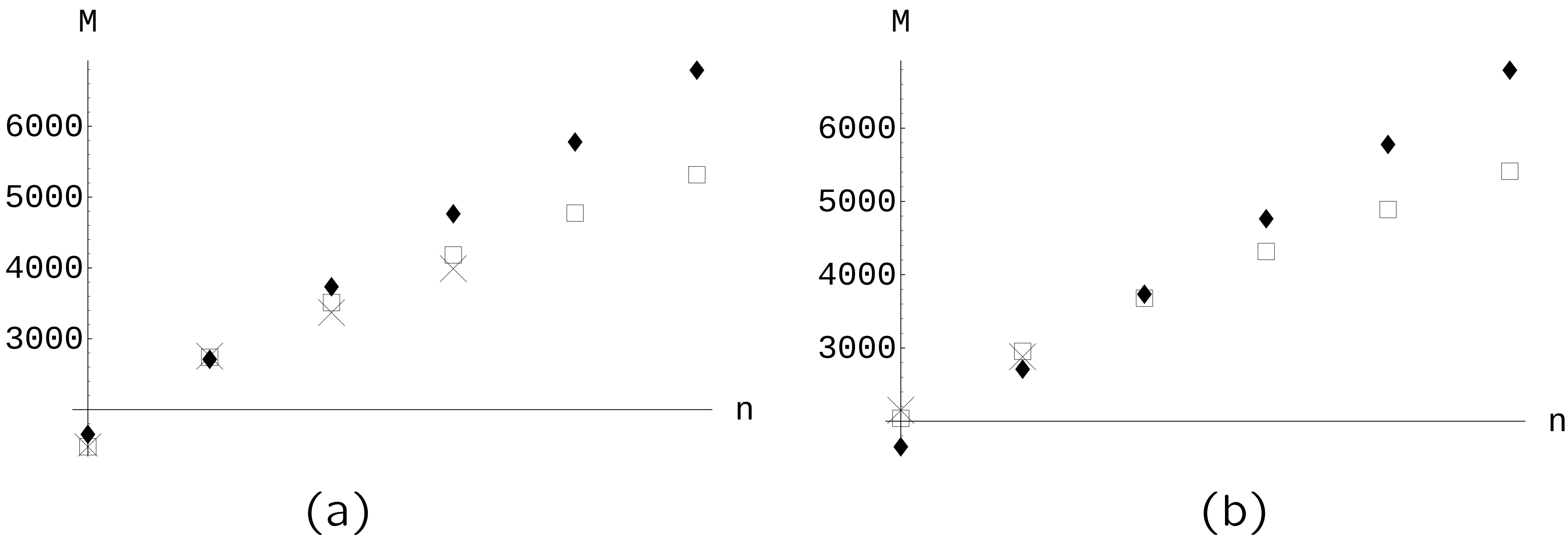

Comparison of glueball spectra from our model with $b_0 = 4.2, l_0 = 0.05$ (boxes), with the lattice QCD data from Ref. I (crosses) and the AdS/QCD computation (diamonds), for (a) 0^{++} glueballs; (b) 2^{++} glueballs. The masses are in MeV, and the scale is normalized to match the lowest 0^{++} state from Ref. I.

The fit to glueball lattice data

J^{PC}	Ref I (MeV)	Our model (MeV)	Mismatch	$N_c \to \infty$	Mismat
0^{++}	**1475 (4%)**	**1475**	0	**1475**	0
2^{++}	2150 (5%)	2055	4%	2153 (10%)	5%
0^{-+}	**2250 (4%)**	**2243**	0		
0^{++*}	**2755 (4%)**	**2753**	0	2814 (12%)	2%
2^{++*}	2880 (5%)	2991	4%		
0^{-+*}	3370 (4%)	3288	2%		
0^{++**}	3370 (4%)	3561	5%		
0^{++***}	3990 (5%)	4253	6%		

Comparison between the glueball spectra in Ref. I and in our model. The states we use as input in our fit are marked in red. The parenthesis in the lattice data indicate the percent accuracy.

Fit and comparison

	HQCD	lattice $N_c = 3$	lattice $N_c \to \infty$	Parameter
$[p/(N_c^2 T^4)]_{T=2T_c}$	**1.2**	**1.2**	-	$V1 = 14$
$L_h/(N_c^2 T_c^4)$	**0.31**	0.28 (Karsch)	**0.31** (Teper+Lucini)	$V3 = 170$
$[p/(N_c^2 T^4)]_{T\to+\infty}$	$\pi^2/45$	$\pi^2/45$	$\pi^2/45$	$M_p\ell = [45\pi^2]^{-1/3}$
$m_{0^{++}}/\sqrt{\sigma}$	**3.37**	3.56 (Chen)	**3.37** (Teper+Lucini)	$\ell_s/\ell = 0.15$
$m_{0^{-+}}/m_{0^{++}}$	**1.49**	**1.49** (Chen)	-	$c_a = 0.26$
χ	$(191 MeV)^4$	$(191 MeV)^4$ (DelDebbio)	-	$Z_0 = 133$
$T_c/m_{0^{++}}$	0.167	-	0.177(7)	
$m_{0^{*++}}/m_{0^{++}}$	1.61	1.56(11)	1.90(17)	
$m_{2^{++}}/m_{0^{++}}$	1.36	1.40(4)	1.46(11)	
$m_{0^{*-+}}/m_{0^{++}}$	2.10	2.12(10)	-	

- G. Boyd, J. Engels, F. Karsch, E. Laermann, C. Legeland, M. Lutgemeier and B. Petersson, *"Thermodynamics of SU(3) Lattice Gauge Theory,"* Nucl. Phys. B **469**, 419 (1996) [arXiv:hep-lat/9602007].

- B. Lucini, M. Teper and U. Wenger, *"Properties of the deconfining phase transition in SU(N) gauge theories,"* JHEP **0502**, 033 (2005) [arXiv:hep-lat/0502003];
"SU(N) gauge theories in four dimensions: Exploring the approach to $N = \infty$," JHEP **0106**, 050 (2001) [arXiv:hep-lat/0103027].

- Y. Chen *et al.*, *"Glueball spectrum and matrix elements on anisotropic lattices,"* Phys. Rev. D **73** (2006) 014516 [arXiv:hep-lat/0510074].

- L. Del Debbio, L. Giusti and C. Pica, *"Topological susceptibility in the SU(3) gauge theory,"* Phys. Rev. Lett. **94**, 032003 (2005) [arXiv:hep-th/0407052].

The pressure from the lattice at different N

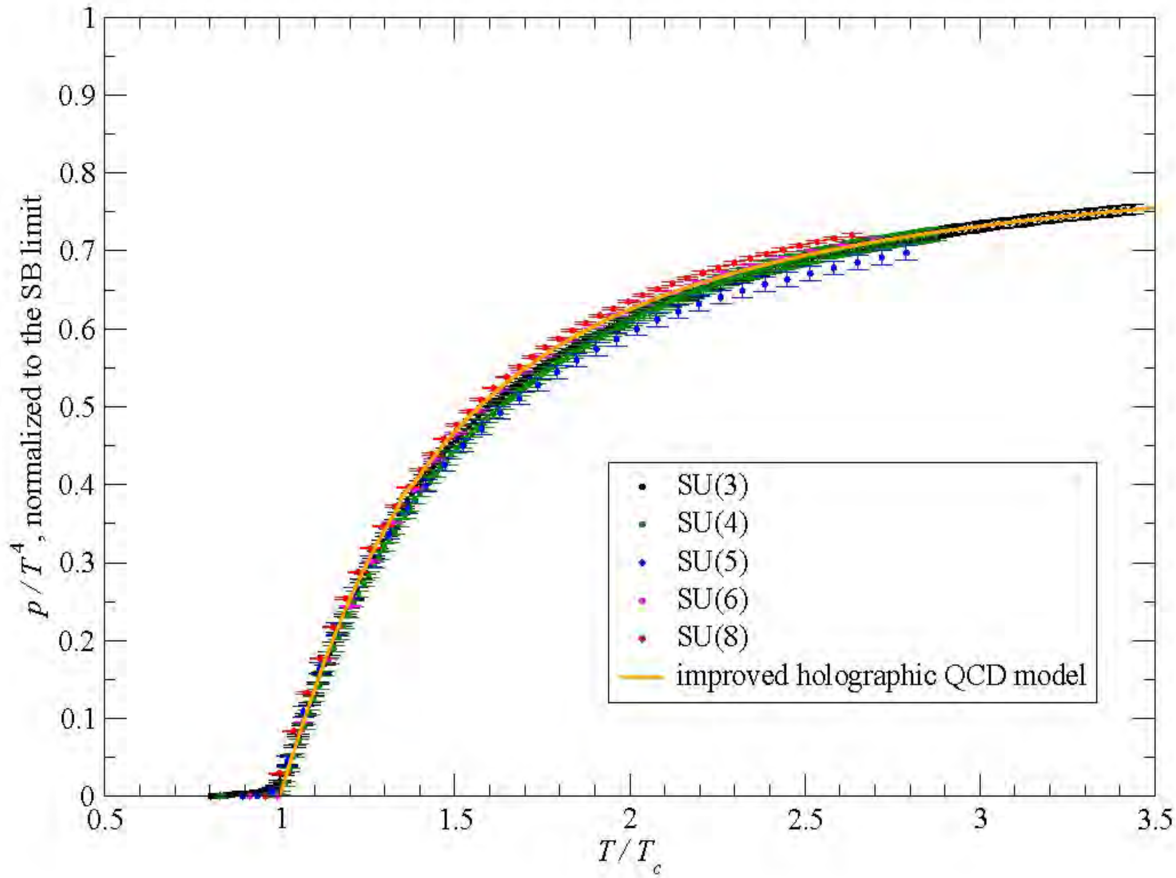

Figure 1: (Color online) The dimensionless ratio p/T^4, normalized to the lattice SB limit $\pi^2(N^2-1)R_I(N_t)/45$, *versus* T/T_c, as obtained from simulations of SU(N) lattice gauge theories on $N_t = 5$ lattices. Errorbars denote statistical uncertainties only. The results corresponding to different gauge groups are denoted by different colors, according to the legend. The yellow solid line denotes the prediction from the improved holographic QCD model from ref. [75] (with a trivial, parameter-free rescaling to our normalization).

Marco Panero arXiv: 0907.3719

The entropy from the lattice at different N

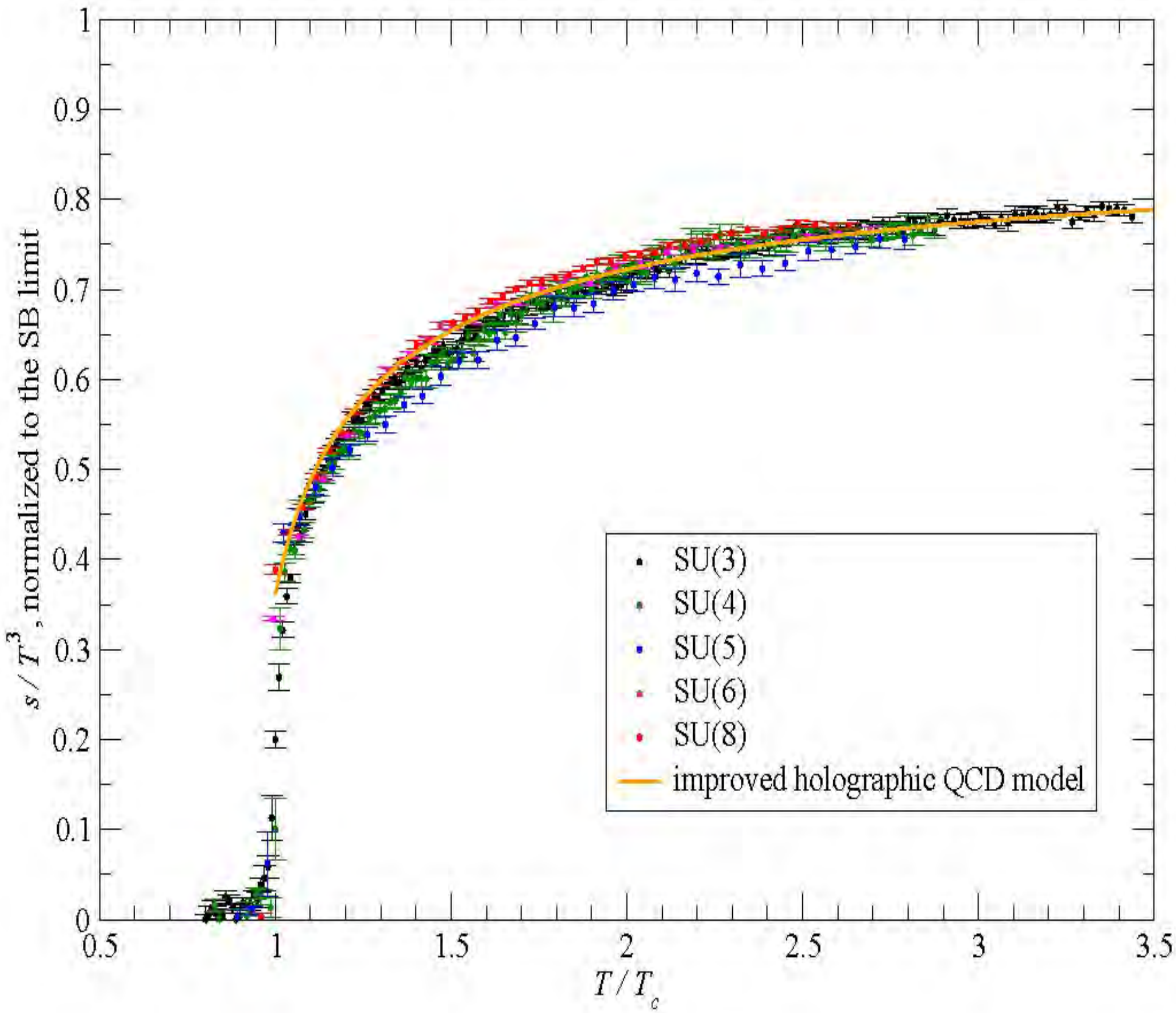

Figure 4: (Color online) Same as in fig. 1, but for the s/T^3 ratio, normalized to the SB limit.

Marco Panero arXiv: 0907.3719

The trace from the lattice at different N

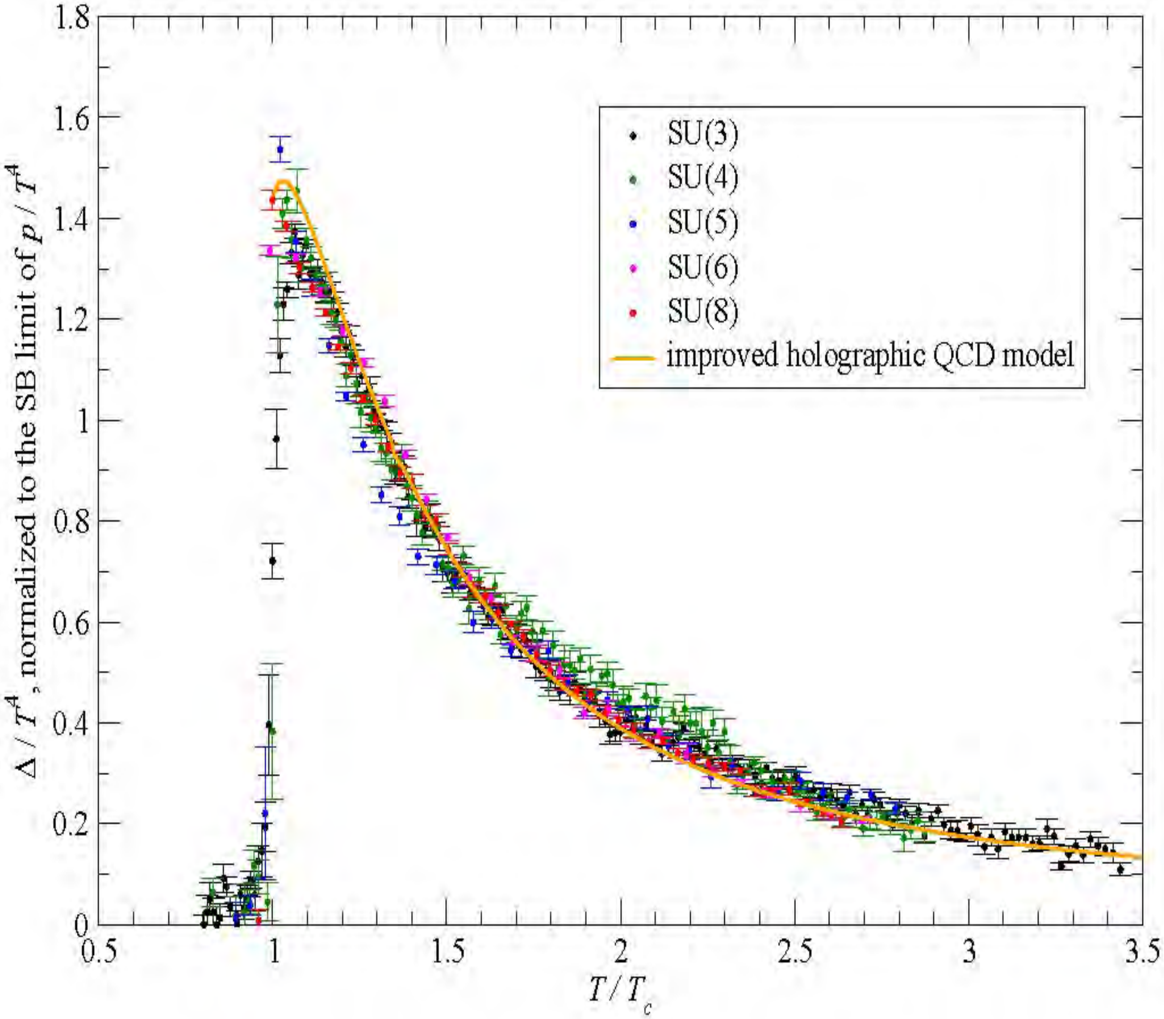

Figure 2: (Color online) Same as in fig. 1, but for the Δ/T^4 ratio, normalized to the SB limit of p/T^4.

Marco Panero arXiv: 0907.3719

The specific heat

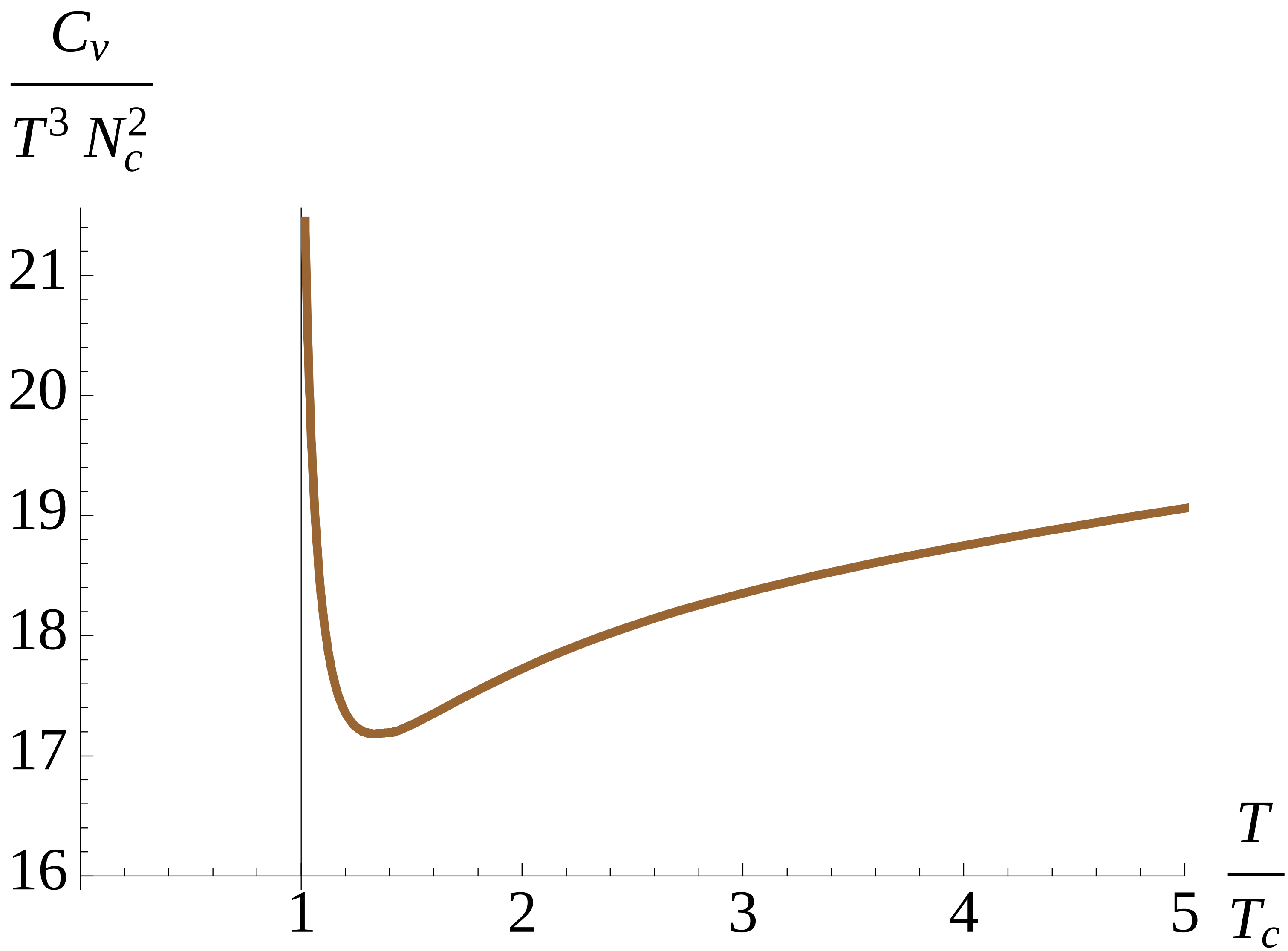

The speed of sound

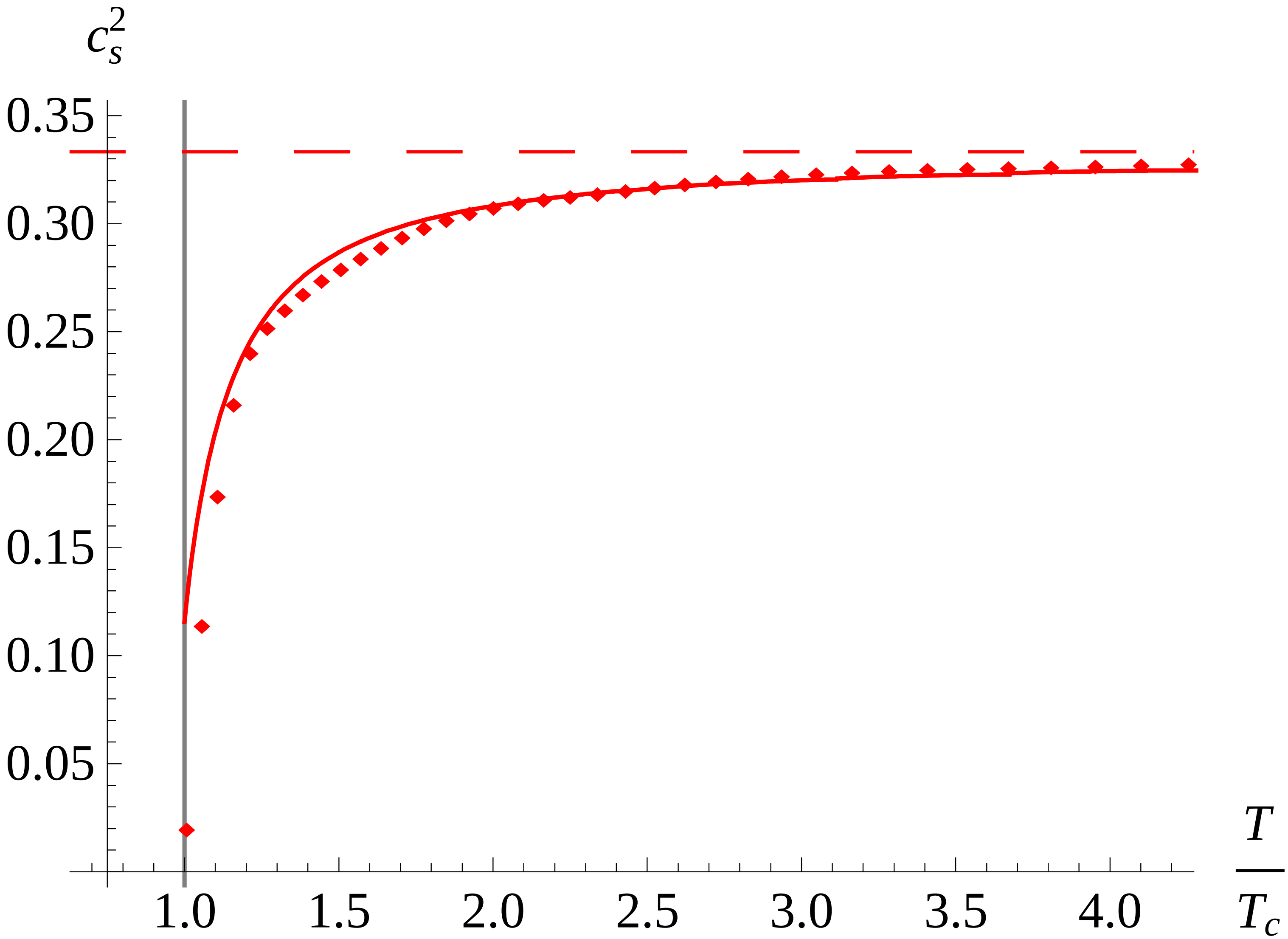

Comparing to Gubser+Nelore's formula

• Gubser+Nelore proposed the following approximate formula for the speed of sound

$$c_s^2 \simeq \frac{1}{3} - \frac{1}{2}\frac{V'^2}{V^2}\Big|_{\phi=\phi_h}$$

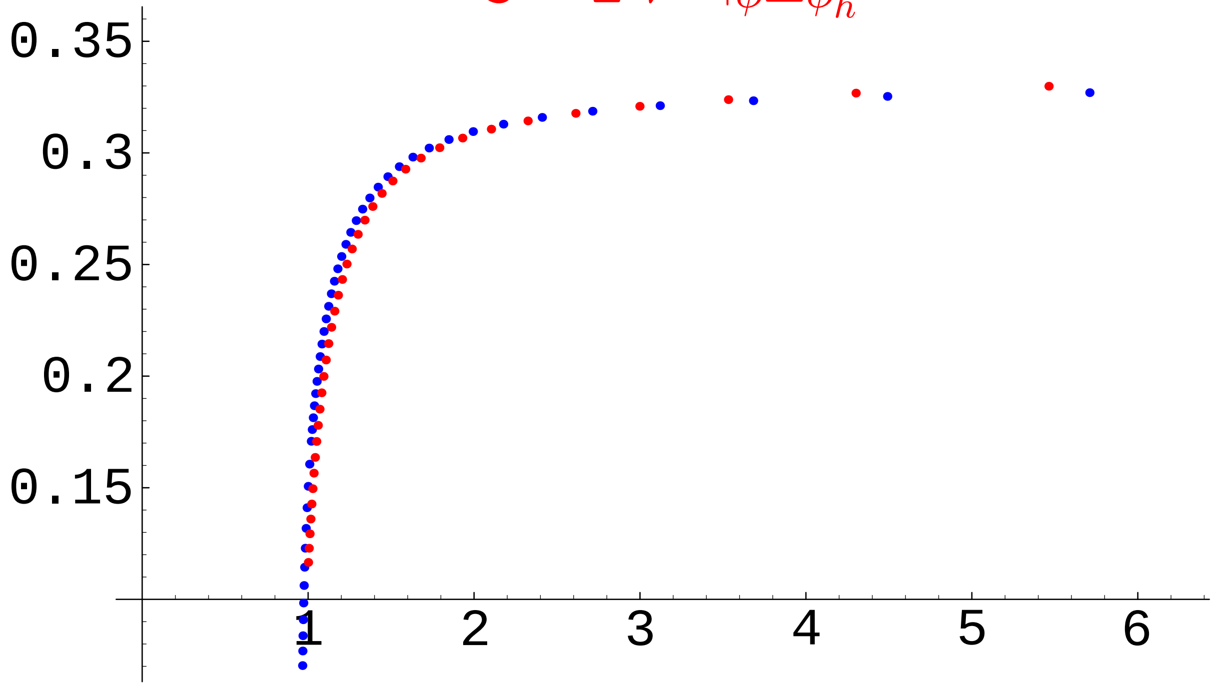

Gursoy (unpublished) 2009

• Red curve=numerical calculation, Blue curve=Gubser's adiabatic/approxima formula.

Detailed plan of the presentation

- Outlook 30 minutes

- The changes of N_{CS} 35 minutes
- The θ RG flow 36 minutes
- The CS spectral function 38 minutes
- Comparison with lattice data (Meyer) 40 minutes
- The fit to glueball lattice data 42 minutes
- Fit and comparison 44 minutes
- The pressure 45 minutes
- The entropy 46 minutes
- The trace 49 minutes
- The free energy 51 minutes
- The specific heat 56 minutes
- The speed of sound 59 minutes
- The Gubser-Nelore formula for c_s 65 minutes